Effect of an adhesive interlayer on the fracture of a brittle coating on a supporting substrate

Jong Ho Kim[a)]
Department of Materials Science and Engineering, Korea Advanced Institute of Science and Technology, Yusong, Taejon 305-701, Korea

Pedro Miranda
Departamento de Electrónica e Ingeniería Electromecánica, Escuela de Ingenierías Industriales, Universidad de Extremadura, 06071 Badajoz, Spain

Do Kyung Kim
Department of Materials Science and Engineering, Korea Advanced Institute of Science and Technology, Yusong, Taejon 305-701, Korea

Brian R. Lawn
Materials Science and Engineering Laboratory, National Institute of Standards and Technology, Gaithersburg, Maryland 20899

(Received 5 August 2002; accepted 31 October 2002)

The role of a compliant adhesive interlayer in determining critical conditions for radial fracture at the undersurfaces of brittle coatings bonded to substrates of dissimilar materials is investigated. Semi-empirical relations for the critical loads are derived by treating the adhesive as part of an effective substrate, thereby reducing the problem to that of a bilayer. A finite-element analysis of a model silicon/epoxy/glass system is used to evaluate adjustable parameters in the analytical relations. *In situ* experimental observations of crack initiation on the same material system are used to verify these relations. The critical loads depend sensitively on the adhesive thickness and modulus. Delamination at the interface in poorly bonded specimens greatly reduces the critical loads. This analysis affords a basis for predicting the prospective fracture resistance of brittle coatings joined by adhesives.

I. INTRODUCTION

Adhesives are commonly used to join plates in laminate structures. Because they are soft and compliant, adhesives can absorb energy from external loads and restrict damage in any one layer from spreading to the next ("crack containment").[1] However, they can also enhance flexural stress states from concentrated loading at the top surface, leading to fracture at the plate interior undersurfaces.[2] This kind of fracture can lead to rapid loss of function, and ultimately failure, of the laminate system. It is considered to be a primary source of failure in dental crowns from occlusal loading of the brittle layer jacket on its dentin support[3–6] and in laminated windows,[7] among other applications.

A problem of general practical interest is the influence of an adhesive interlayer on the loads to initiate transverse radial cracking at the undersurface of a brittle coating adhesively bonded to a supporting substrate of different material, subject to a concentrated load at the top surface. Chai and Lawn[8] considered the special case of an epoxy adhesive between two like glass plates and derived working relations for the critical loads for radial fracture in terms of adhesive thickness and modulus mismatch. (Near-contact cone cracking at the top glass surface was shown to be a competitive fracture mode only in extreme cases of very thick coatings or sharp contacts.) The question arises as to the role of substrate/coating elastic modulus mismatch, as well as substrate/adhesive mismatch and adhesive thickness, in the critical conditions for radial cracking.

In this paper we examine these critical conditions in model coating/adhesive/substrate systems. Silicon/epoxy/glass is used as a case study, i.e., the same configuration considered by Chai and Lawn but with the upper glass layer replaced by silicon.[9] Silicon and glass have sufficiently different moduli that mismatch effects

[a)]The present work was done at Materials Science and Engineering Laboratory, National Institute of Standards and Technology, Gaithersburg, Maryland 20899.

should be apparent. Also, unlike glass, silicon is relatively immune to slow crack growth, so that any kinetic effects in the ensuing experimental critical load data (strongly apparent in glass/epoxy bilayer systems[9]) may be minimized. Retention of glass as the substrate enables *in situ* observations of radial cracking during loading.[2] For analysis, a finite element algorithm is used to determine tensile stresses at the silicon undersurfaces beneath concentrated surface loads as a function of the applied load. A semi-empirical relation for the effective modulus of the composite adhesive/glass underlayer is then derived from fits to the finite element analysis (FEA) data in terms of relative moduli and adhesive thickness. Expressions for the critical loads for radial cracking in the silicon coating are obtained as a function of adhesive thickness (relative to coating thickness) and elastic modulus ratios by equating the maximum tensile stresses to the bulk strength of the coating material. Experiments on silicon/adhesive/glass laminates are conducted to test these relations. The prospect of using the analysis as a means for characterizing adhesive properties in the special context of layer structures is discussed.

II. THEORY

A. Stress analysis

Consider a coating of thickness d and modulus E_c bonded by an adhesive interlayer of thickness h and modulus E_i to a thick substrate of modulus E_s [Fig. 1(a)]. Generally, $E_i < E_s$ and $E_i < E_c$, but there is no restriction on the relative values of E_c and E_s. The system is loaded at its top surface with a spherical indenter at load P. Loading conditions are such that the contact dimensions remain small compared with the coating thickness. We wished to determine how the critical load P_R for transverse radial cracking in the coating varies with relative moduli and layer thicknesses.

Suppose that the tensile stresses at the undersurface of the coating (Fig. 1) can be described (if only approximately) by a well-documented relation for a flexing plate on an elastic foundation,[10] but with modification to allow for incorporation of the adhesive:

$$\sigma = (P/Bd^2)\log(E_c/E^*) \quad , \tag{1}$$

where B is a dimensionless constant and $E^* = E^*(h/d, E_s/E_i)$ is an effective modulus of the composite adhesive/substrate underlayer in accordance with the following boundary conditions: $E^* = E_s$ at $h = 0$ [coating/substrate bilayer limit, Fig. 1(b)]; and $E^* = E_i$ at $h \to \infty$ or $E_s = E_i$ [coating/adhesive bilayer limit, Fig. 1(c)]. A simple, empirical function that meets these bounding requirements and has some basis in contact mechanics[11] is

$$E^* = E_i(E_s/E_i)^L \quad , \tag{2}$$

with the dimensionless function $L = L(h/d)$ in the range $0 \leqslant L \leqslant 1$ to be determined. This last relation is slightly different from another empirical function used in an earlier study[8] but is preferred because it is simpler and accommodates all relative values of E_c/E_s.

The form of Eq. (1) has been verified in the bilayer limit $E^* = E_s$ (or $E^* = E_i$).[12] To test the suitability of Eq. (2) in the more general usage of Eq. (1), we conduct FEA of stresses in our model silicon/epoxy/glass trilayer system in the indentation configuration of Fig. 1(a), using elastic constants for the constituent materials from a previous paper.[9] Details of the FEA algorithm have been previously described.[13] It is assumed that the interfaces remain fully bonded at all stages of the computation. In our calculations the quantities $d = 1$ mm and $E_c = 170$ GPa (silicon) are held fixed, and other quantities are varied. The contact radius satisfies the condition $a < d/4$ (Fig. 1) in all cases, justifying a point-contact approximation for the loading. Dimensionless, invariant quantities $S_t = (\sigma d^2/P)_t$ are determined for each specified coating/adhesive/substrate trilayer combination by

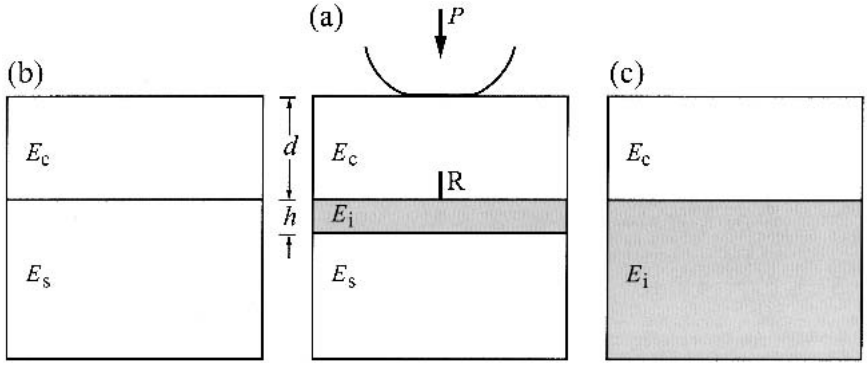

FIG. 1. Schematic drawing of coating of thickness d and modulus E_c bonded by an adhesive interlayer of thickness h and modulus E_i to a thick substrate of modulus E_s, in contact with indenter at load P at top surface: (a) coating/adhesive/substrate system, (b) coating/substrate bilayer limit, (c) coating/adhesive bilayer limit. R is trace of the radial crack.

best fitting to FEA data for $\sigma(P)$. Imposition of the bilayer limit $S_b = (\sigma d^2/P)_b$ at $h \to \infty$ [Fig. 1(c)] provides a useful reference state. Using this state as a boundary condition, inversion of Eq. (1) then yields $E^* = E_i(E_s/E_i)^{(1-S_t/S_b)}$, from which E^* may be evaluated without specific knowledge of B in Eq. (1). In Fig. 2, E^*/E_i is plotted as a function of h/d for fixed $E_i = 3.5$ GPa (epoxy) and selected values of E_s. Likewise, in Fig. 3 E^*/E_i is plotted as a function of E_s/E_i for fixed $E_s = 70$ GPa (glass) and selected values of h. The FEA data in these plots can be deconvoluted to obtain L as a function of h/d in Fig. 4, which can be fitted to a Weibull function[11]

$$L = \exp\{-[\alpha + \beta\log(h/d)]^\gamma\} \quad . \tag{3}$$

Such a fit yields $\alpha = 1.18$, $\beta = 0.33$, and $\gamma = 3.13$. The solid curves in Figs. 2 and 3 are regenerations of Eqs. (1–3) using these parameter fits. There are systematic variations between these curves and the FEA data sets in these figures, indicating a lack of universality of Eq. (2). Nevertheless, the equations accommodate the main data trends over a broad range of variables, except at large E_s and small h/d.

B. Critical loads for radial cracking

Now consider the critical conditions to produce radial cracking. Suppose that such cracking initiates from a prepresent flaw at the coating undersurface when the tensile stress in Eq. (1) just equals the bulk strength of the coating material, i.e., $\sigma = \sigma_c$, corresponding to a critical load $P = P_R$. This will remain a good approximation as long as the flaw size remains small compared to the thickness d (see Sec. III. A).[2] Then we obtain from Eqs. (1) and (2)

$$P_R = B\sigma_c d^2/\log(E_c/E^*) = P^*/\{\log(E_c/E_i) - L\log(E_s/E_i)\} \quad , \tag{4}$$

where $P^* = B\sigma_c d^2$ is a convenient normalization load combining the coating strength and thickness properties. Note that there is no restriction on E_c/E_s in this scheme; i.e., E_c can be larger or smaller than E_s.

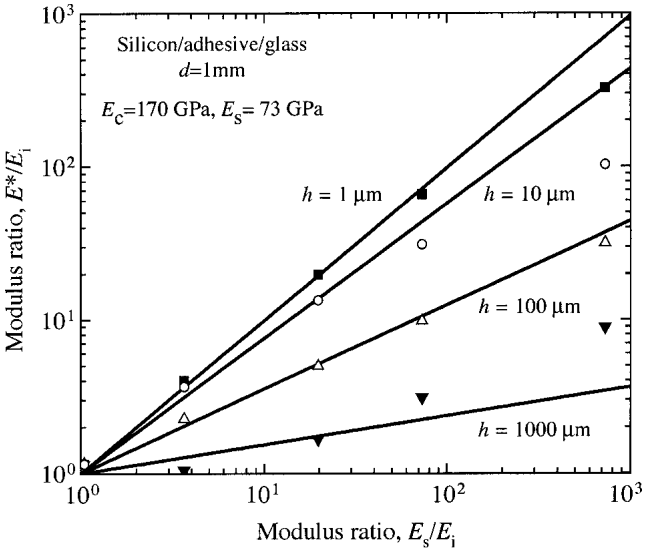

FIG. 3. FEA data for E^*/E_i as a function of E_s/E_i for fixed $E_s = 70$ GPa (glass) and selected values of h. Solid curves are fits to Eqs. (1–3).

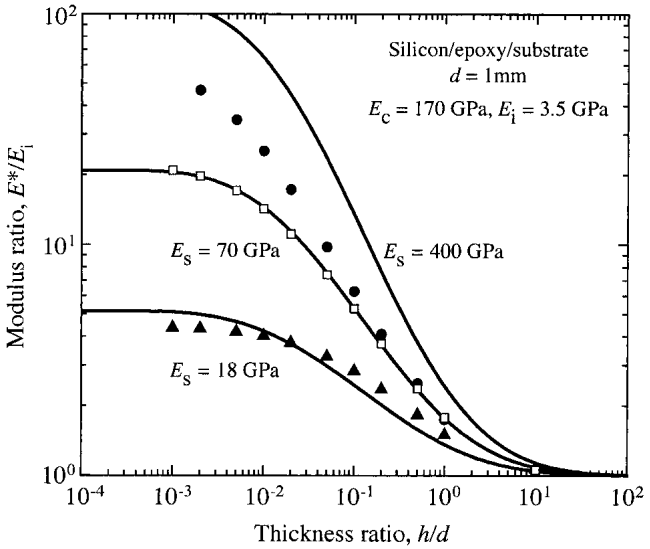

FIG. 2. FEA data for E^*/E_i as a function of h/d for fixed $E_i = 3.5$ GPa (epoxy) and selected values of E_s. Solid curves are fits to Eqs. (1–3).

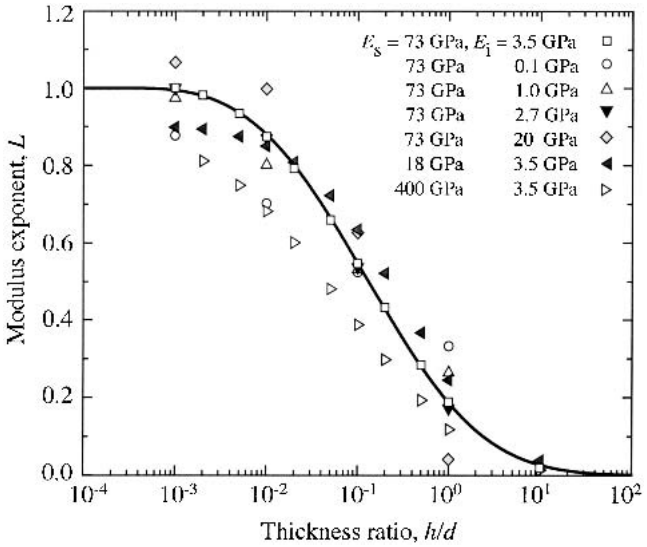

FIG. 4. Plot of L as a function of h/d in Eq. (3), using FEA data from Figs. 2 and 3.

III. EXPERIMENTS

A. Materials and testing

Layer structures were prepared from polished (001) monocrystalline silicon plates of thickness $d = 1$ mm and lateral dimensions 75×25 mm (Virginia Semiconductors, Fredericksburg, VA) and soda-lime glass plates 5 mm thick with the same lateral dimensions. The silicon undersurfaces were lightly abraded with grade 600 SiC grit to introduce controlled flaws for ensuing radial cracking.[2,9] These flaws were typically <10 μm (compare $d = 1$ mm), so the assumption of a critical stress condition for fracture remains a good approximation. Adhesives were then used to bond the silicon coating layers to the glass base substrates, using spacers to predetermine the adhesive thickness h, and allowed to cure in air for two days. Epoxy thicknesses between 5 μm and 2 mm were used in our experiments. A list of the adhesives used is given in Table I. The glass and silicon surfaces were pretreated with a silane coupling agent (3-methacryloxypropyltrimethoxysilane) to improve the ensuing bonding. Dummy specimens of the adhesive materials were cast in molds for measurement of Young's modulus using an acoustic impulse excitation apparatus (Grindosonic MK5, J.W. Lemmens Inc., St. Louis, MO).

The silicon/adhesive/glass trilayers were subjected to top-surface contact loading from a tungsten carbide indenting sphere (radius 3.96 mm) mounted into the crosshead of a mechanical loading machine (Model 5500R, Instron Corp, Canton, MA). Several tests were made on any one bilayer surface. The onset of radial cracking in the coating undersurface was viewed from below using an axially aligned microscope zoom system (Zoom 100D, Optem, Santa Clara, CA) mounted into a video camcorder (Canon XL1, Canon, Lake Success, NY), enabling direct measurement of critical loads P_R. The critical load could also be determined from distinct drops in the Instron load data output[9] or by acoustic signals from a piezoelectric transducer (Mistras 2001, Physical Acoustics Corp., Princeton, NJ),[12] useful adjuncts for opaque or semi-opaque adhesives. For most adhesives the interlayer interface remained intact up to and beyond the critical load P_R for radial cracking; for some, premature delamination occurred during the testing prior to P_R, usually at the silicon/adhesive interface. For still others, the delamination occurred either during normal handling before testing or immediately on first application of the contact load.

B. Critical load data for model adhesive system

In Fig. 5 experimental data are plotted for the critical loads P_R to produce transverse radial cracking in silicon coatings on glass substrates in well-bonded (nondelaminated) specimens, as a function of adjoining epoxy adhesive thickness h, for fixed $d = 1$ mm (loading rate $\approx 10\ \mathrm{Ns}^{-1}$). Horizontal dashed lines are bilayer limits, silicon/glass at $h = 0$ and silicon/epoxy at $h = \infty$, evaluated from Eq. (4). In Fig. 6 analogous P_R data are plotted as a function of adhesive modulus E_i for fixed $h/d = 0.15$. The data points are means and standard deviations. Solid curves are computations from Eq. (4), using a best-fit adjustment $P^* = 421$ N. The computed curves do not intersect all the data points, with discrepancies up to 25% in extreme cases, but nevertheless reproduce the main trends.

As indicated, some specimens delaminated during or even prior to loading, with attendant reduction in P_R. To quantify the effects of such events, Fig. 7 shows values of P^* for all adhesive systems tested, evaluated by inserting measured P_R values into Eq. (4) along with E_i, E_c, and E_s from modulus measurements and L from the calibrated Eq. (3). Specimens that remained fully bonded throughout the test cycle are indicated by the fully shaded bars; those that delaminated partially during loading by partially shaded bars; and those that delaminated completely before testing by unshaded bars. In all cases, regardless of any delamination, loading was continued until the critical value P_R was attained. The quantity $P^* = B\sigma_c d^2$ in Eq. (4) may be interpreted as an effective breaking force for the coating. Thus weak interfaces can be highly deleterious to the strength properties of coating systems.

TABLE I. Young's modulus of materials used in this study.

Name	Material type	Supplier	Modulus E_i (GPa)
Epoxy (soft)	Polymer resin	Harcos Chemicals, Bellesville, NJ	2.8
Epoxy	Polymer resin	Harcos Chemicals, Bellesville, NJ	3.7
Cavitec	Zinc oxide eugenol	Kerr Corp., Romulus, MI	0.28
Dycal	Calcium hydroxide	Dentsply, Milford, DE	4.1
Durelon	Polycarboxylate cement	ESPE America, Norristown, PA	8.3
VarioLink II	Resin-based cement	Ivoclar Vivadent, Liechtenstein	8.6
GC Fuji I	Glass ionomer cement	GC Corporations, Tokyo, Japan	4.6
Fleck's cement	Zinc phosphate	Mizzy Inc., Cherry Hill, NJ	10.9
Rely X	Resin modified glass ionomer	3M Dental Products, St. Paul, MN	3.1

IV. DISCUSSION

Compliant interlayers between a coating and dissimilar substrate can result in transverse radial cracks from concentrated loading at the top surface (Fig. 1). The critical loads P_R for this deleterious cracking mode diminish as the interlayer thickness increases and modulus decreases. (At the other end of the spectrum, as the interlayer thickness decreases, the FEA-computed stress intensity within the adhesive increases, raising the prospect of yield and consequent reduction in P_R.[13]) Coating thickness and strength are also factors in the critical conditions via P^*. Interfacial bonding is another critical factor; delamination not only detaches the coating from the substrate, but allows the outer annular coating regions to displace upward, enhancing flexure immediately below the contact and thus strongly diminishing P_R.[14] Figures 5–7 quantify the considerable threat to the integrity of layer structures posed by thick, compliant, and debonding adhesives, respectively. Thus in Fig. 5, an increase in adhesive thickness from $h = 10$ μm to $h = 1$ mm produces a fourfold decrease in P_R; in Fig. 6, an increase in adhesive modulus from $E_i = 1$ GPa produces a twofold increase in P_R; and in Fig. 7, delamination produces as much as a fourfold decrease in P_R. For damage prevention, thin, stiff, well-bonded adhesives are prime requirements.

Equations for the critical loads P_R were derived as functions of relative elastic moduli and layer thickness for coating/adhesive/substrate systems with well-bonded interfaces. These equations account for the main trends in the finite-element method and experimental data for our model silicon/adhesive/glass layer system. As such, they provide a quantitative basis for characterizing adhesives. At the same time, systematic discrepancies as much as 25% are evident in the data fits, particularly in the regions of small h and large E_s. This level of uncertainty in the data fits, coupled with the semi-empirical nature of the relations, indicates that care needs to be exercised in any extrapolation outside the current data range of *h/d,*

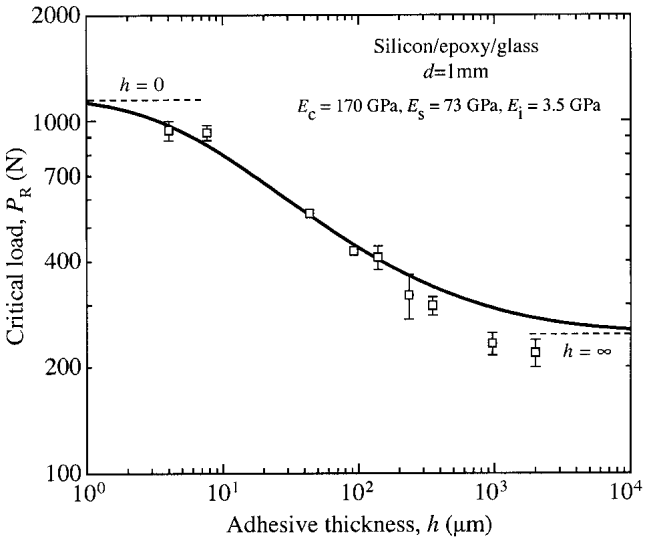

FIG. 5. Experimental data showing critical load P_R for radial cracking in silicon coating bonded to glass substrate with epoxy adhesive, as function of adhesive thickness h for $d = 1$ mm. Horizontal dashed lines are bilayer limits, silicon/glass at $h = 0$ and silicon/epoxy at $h = \infty$.

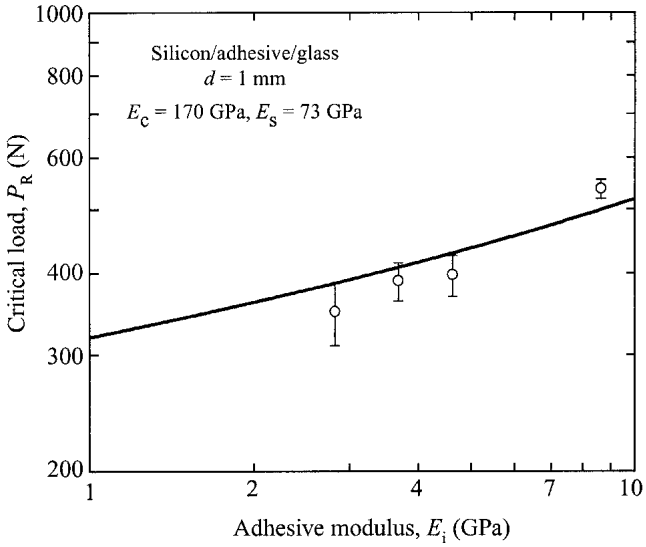

FIG. 6. Experimental data showing critical load P_R for radial cracking in silicon coating on glass substrate as function of adhesive modulus E_i, for $h = 150$ μm, $d = 1$ mm. Only data for well-bonded adhesives are included in this plot.

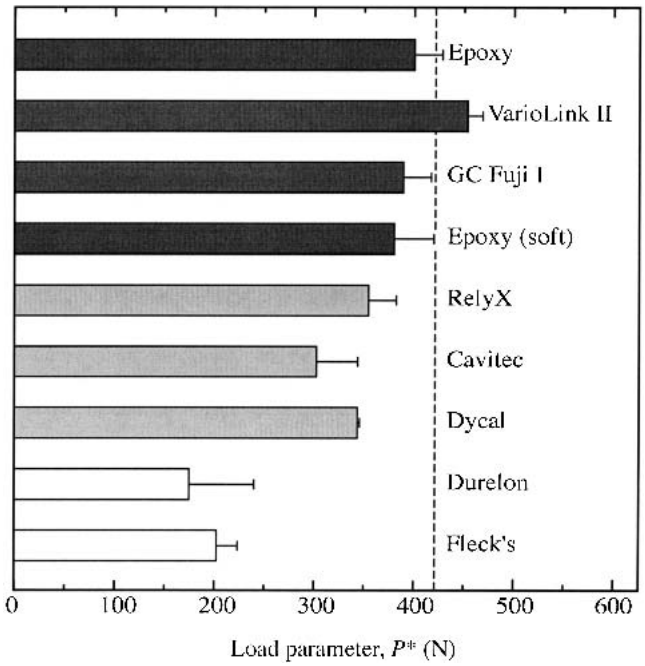

FIG. 7. Experimental data showing quantity P^* for silicon coating on glass substrate, for different substrates, fixed $d = 1$ mm. Fully shaded bars indicate well-bonded specimens, partially shaded bars indicate delamination during loading, and unshaded bars indicate delamination prior to loading.

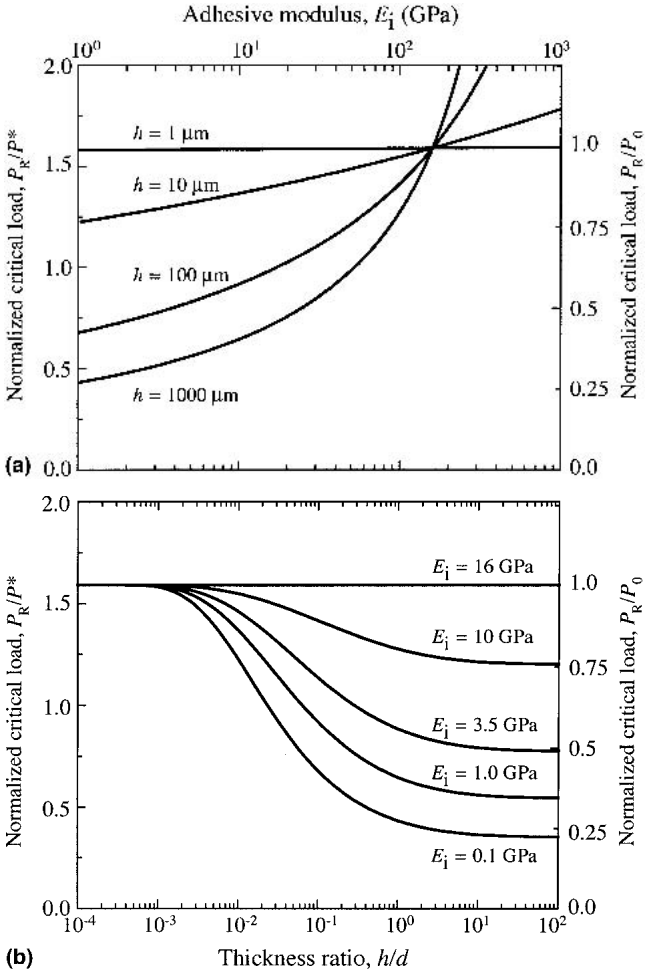

FIG. 8. Predicted dependence of P_R for porcelain (E_c = 68 GPa) of fixed thickness d = 1.5 mm on dentin (E_s = 16 GPa), as function of (a) adhesive modulus E_i at selected values of h and (b) adhesive thickness h at selected values of E_i.

E_s/E_i and E_c/E_i. Other factors can affect the effective strength σ_c relative to the bulk strength of the coating material, and hence the quantity $P^* = B\sigma_c d^2$ defined in conjunction with Eq. (4): delamination, by activating premature failures; rate effects, from slow crack growth in the coating (not a factor here, but most likely in most other ceramic-coating systems, e.g., in glassy porcelain coatings) or creep in the adhesive;[9] residual stresses, from shrinkage or expansion of the adhesive during curing;[15] flaw statistics, by limiting the density and size of critical flaws in the immediate contact zone.[16] It is for this reason that we simply regard P^* as an adjustable quantity in our data fitting in Figs. 5 and 6.

Notwithstanding the sources of potential discrepancy listed above, the equations in Sec. II may be used to make comparative *a priori* predictions for prospective coating/adhesive/substrate systems. We illustrate here by using these equations to predict critical loads for a hypothetical porcelain coating (E_c = 68 GPa) of thickness d = 1.5 mm bonded onto dentin (E_s = 16 GPa) with hypothetical dental cements of variable modulus and thickness. Accordingly, Fig. 8 shows P_R/P^* from Eq. (4) as a function of (a) adhesive modulus E_i at selected values of h, and (b) adhesive thickness h at selected values of E_i, for porcelain thickness d = 1.5 mm. Also plotted on the right axis is the quantity P_R/P_0, where P_0 is the critical load for radial cracking in an ideal porcelain/dentin bilayer with h = 0, to emphasize the degrading influence of the adhesive. The variation in P_R can be significant over the clinically relevant range (E_i = 3 to 20 GPa, h = 10 to 100 μm), more so as E_i diminishes below the modulus of dentin and as h increases. As always, it is crucial to ensure good bonding at the adhesive interfaces to avoid further reduction in P_R. These results can be taken as useful guidelines for dentists and technicians in the preparation of dental crowns and other prosthetic devices.

ACKNOWLEDGMENTS

Thanks are due to Mariano Polack and Yan Deng for discussions on dental adhesives. This study was supported by internal funds from the National Institute of Standards and Technology (NIST) and from the Korea Ministry of Education (Brain Korea 21 Program of Korea Advanced Institute of Science and Technology), and by grants from the United States National Institute of Dental and Craniofacial Research (Grant No. PO1 DE10976), and the Junta de Extremadura-Consejeria de Educacion Ciencia y Tecnologia y el Fondo Social Europeo, Spain (Grant No. IPR00A084). Information on product names and suppliers does not imply endorsement by NIST.

REFERENCES

1. W.J. Clegg, K. Kendall, N.M. Alford, T.W. Button, and J.D. Birchall, Nature **347,** 455 (1991).
2. H. Chai, B.R. Lawn, and S. Wuttiphan, J. Mater. Res. **14,** 3805 (1999).
3. S.S. Scherrer and W.G.d. Rijk, Int. J. Prosthodont **6,** 462 (1993).
4. S.S. Scherrer, W.G.d. Rijk, U.C. Belser, and J-M. Meyer, Dent. Mater. **10,** 172 (1994).
5. J.R. Kelly, J. Prosthet. Dent. **81,** 652 (1999).
6. B.R. Lawn, Y. Deng, and V.P. Thompson, J. Prosthet. Dent. **86,** 495 (2001).
7. S.J. Bennison, A. Jagota, and C.A. Smith, J. Am. Ceram. Soc. **82,** 1761 (1999).
8. H. Chai and B.R. Lawn, J. Mater. Res. **15,** 1017 (2000).
9. C-S. Lee, D.K. Kim, J. Sanchez, P. Miranda, A. Pajares, and B.R. Lawn, J. Am. Ceram. Soc. **85,** 2019 (2002).
10. S. Timoshenko and S. Woinowsky-Krieger, *Theory of Plates and Shells* (McGraw-Hill, New York, 1959).
11. X.Z. Hu and B.R. Lawn, Thin Solid Films **322,** 225 (1998).
12. Y-W. Rhee, H-W. Kim, Y. Deng, and B.R. Lawn, J. Am. Ceram. Soc. **84,** 1066 (2001).
13. P. Miranda, A. Pajares, F. Guiberteau, F.L. Cumbrera, and B.R. Lawn, J. Mater. Res. **16,** 115 (2001).
14. T.J. Lardner, J.E. Ritter, and G-Q. Zhu, J. Am. Ceram. Soc. **80,** 1851 (1997).
15. C. Leevailoj, J.A. Platt, M.A. Cochran, and B.K. Moore, J. Prosthet. Dent. **80,** 699 (1998).
16. P. Miranda, A. Pajares, F. Guiberteau, F.L. Cumbrera, and B.R. Lawn, Acta Mater. **49,** 3719 (2001).